



## Molecular Crystals and Liquid Crystals

Publication details, including instructions for authors and subscription information:

<http://www.tandfonline.com/loi/gmcl20>

### Effect of Mixed Cellulose Ester Membrane Structure on Appearance of Cholesteric Blue Phases

Masayoshi Ojima<sup>a</sup>, Takeshi Noma<sup>a</sup>, Hiroaki Asagi<sup>a</sup>, Akihiko Fujii<sup>a</sup>, Masanori Ozaki<sup>a</sup> & Hirotsugu Kikuchi<sup>b</sup>

<sup>a</sup> Grad. School of Engineering, Osaka University, Suita, Osaka, Japan

<sup>b</sup> Institute for Materials Chemistry and Engineering, Kyusyu University, Kasuga, Fukuoka, Japan

Version of record first published: 05 Oct 2009

To cite this article: Masayoshi Ojima, Takeshi Noma, Hiroaki Asagi, Akihiko Fujii, Masanori Ozaki & Hirotsugu Kikuchi (2009): Effect of Mixed Cellulose Ester Membrane Structure on Appearance of Cholesteric Blue Phases, *Molecular Crystals and Liquid Crystals*, 512:1, 136/[1982]-142/[1988]

To link to this article: <http://dx.doi.org/10.1080/15421400903050723>

PLEASE SCROLL DOWN FOR ARTICLE

Full terms and conditions of use: <http://www.tandfonline.com/page/terms-and-conditions>

This article may be used for research, teaching, and private study purposes. Any substantial or systematic reproduction, redistribution, reselling, loan,

sub-licensing, systematic supply, or distribution in any form to anyone is expressly forbidden.

The publisher does not give any warranty express or implied or make any representation that the contents will be complete or accurate or up to date. The accuracy of any instructions, formulae, and drug doses should be independently verified with primary sources. The publisher shall not be liable for any loss, actions, claims, proceedings, demand, or costs or damages whatsoever or howsoever caused arising directly or indirectly in connection with or arising out of the use of this material.

## Effect of Mixed Cellulose Ester Membrane Structure on Appearance of Cholesteric Blue Phases

Masayoshi Ojima<sup>1</sup>, Takeshi Noma<sup>1</sup>, Hiroaki Asagi<sup>1</sup>,  
Akihiko Fujii<sup>1</sup>, Masanori Ozaki<sup>1</sup>, and  
Hirotsugu Kikuchi<sup>2</sup>

<sup>1</sup>Grad. School of Engineering, Osaka University, Suita, Osaka, Japan

<sup>2</sup>Institute for Materials Chemistry and Engineering,  
Kyusyu University, Kasuga, Fukuoka, Japan

*Temperature range of cholesteric blue phase (BP) was expanded by infiltrating liquid crystal (LC) that exhibits blue phases into mixed cellulose ester membrane (MCEM). The expansion of the BP temperature range was induced by pinning effect on the network surfaces of membrane. In particular, the temperature range of BP I in the LC/MCEM composite is four times wider than that of pure BP LC compound. Solvent treatment of MCEM with aqueous solution of ethanol leads thinner network of MCEM and bigger expansion of BP I temperature range. Polarizing microscopic observations and reflection spectrum measurements of the expanded BP have been carried out. Cooling rate dependence of the BP temperature range was also investigated, which indicated that the expansion of the BP temperature range upon infiltrating LC into MCEM was induced by the pinning effect at network surfaces in the MCEM.*

**Keywords:** cholesteric blue phase; membrane; mixed cellulose ester; pinning effect

## INTRODUCTION

The cholesteric blue phases (BPs) have three-dimensional (3D) helical structures in temperature range between a chiral nematic phase and an isotropic liquid phase, and exhibit many unique characteristics [1]. Their 3D structures have the lattice constant in the order of visible wavelength and include regularly ordered disclinations resulting from

We acknowledge Chisso Co. Ltd. for kindly providing the nematic liquid crystal material.

Address correspondence to Masayoshi Ojima, Grad. School of Engineering, Osaka Univ. 2-1 Yamada-oka, Suita, Osaka, Japan. E-mail: [mojima@opal.eei.eng.osaka-u.ac.jp](mailto:mojima@opal.eei.eng.osaka-u.ac.jp)

the 3D helicoidal molecular alignment [2,3]. From the viewpoint of display application, since BPs are optically isotropic, display devices based on them should have a wide view angle and should not require an alignment process. In addition, because of their 3D helical structure with a periodicity in the order of visible wavelength, applications to photonic crystals [4–6] and fast electro-optical modulation [7–9] are also expected.

Despite their potential applications, BPs appear in very narrow temperature range because of the inevitable existence of disclination. Recently, several attempts have been proposed to widen the temperature range of the BPs, which describe the stabilizations of the 3D cubic lattice by polymerizing disclination lines [10], and by using a flexoelectricity of twin molecules [11] and a chiral compound possessing molecular biaxiality [12]. We have proposed also the stabilization by infiltrating BPs in 3D polymer network structure which is formed by a polymerization-induced phase separation of the liquid crystal – pre-polymer mixture [13]. These synthesize atmosphere leads to obscure mechanism of stabilization of BPs. It is well known that bulk phase transitions are significantly alerted in the network structure or thin film, and the quenched disorder cause these behavior [14–16]. In this study, the temperature range of the BP infiltrated in MCEM was discussed. Solvent treatment effect was also discussed in this study.

## EXPERIENCE

Figure 1 shows the scanning electron microscope (SEM) images of MCEM having 3- $\mu\text{m}$  and 0.3- $\mu\text{m}$  pore size. The LC materials used in this study comprised a nematic mixture (JC-1041XX, Chisso Co.) and 4-cyano-4'-pentylbiphenyl (5CB). A chiral dopant (ISO-(6OBA)<sub>2</sub>)

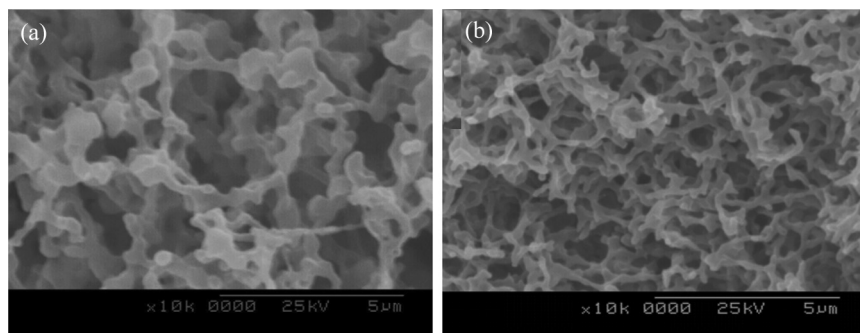


**FIGURE 1** SEM images of MCEM (a) 3  $\mu\text{m}$  and (b) 0.3  $\mu\text{m}$ .

**TABLE 1** Constituent Fraction of the BP and the Phase-Transition Temperatures

LC mixture		Chiral dopant	
5CB (wt%)	JC 1041 XX (wt%)	ISO-(60BA) <sub>2</sub> (wt%)	Phase transition temperature
46.5	46.5	7.0	Ch-42.3-BP I-44.0-BP II-45.2-ISO

was used to induce the BPs and a cholesteric phase. The constituent fractions and the phase-transition temperatures of the LC are listed in Table 1. The LC materials were infiltrated into the MCEM in vacuumed chamber.

Aqueous solution of ethanol (5 wt%) was used to investigate solvent treatment effect on MCEM structure and appearance temperature range of BPs. Aqueous solution of ethanol penetrated through MCEM for 5 s, and then MCEM was dried in vacuumed chamber at 90°C. LC was also infiltrated in MCEM after the solvent treatment and dry process in vacuumed chamber.

The optical textures of the samples (BP infiltrated in MCEM and BP only) were observed by a polarizing optical microscope (Nikon) equipped with a hot stage (METTLER, FP90). The reflection spectrum of the samples was measured with a multichannel photodetector (Hamamatsu photonics C7473-36).

RESULTS AND DISCUSSION

Polarizing optical microscope observations can show characteristic textures apparently associated with different kinds of liquid crystal phases. Figure 2 shows the optical texture of the LC infiltrated in 1-μm MCEM. The sample was cooled from the isotropic phase at a cooling rate of 1.0°C/min. It is well known that there are three thermodynamically stable blue phases, BP I, BP II and BP III, occurring

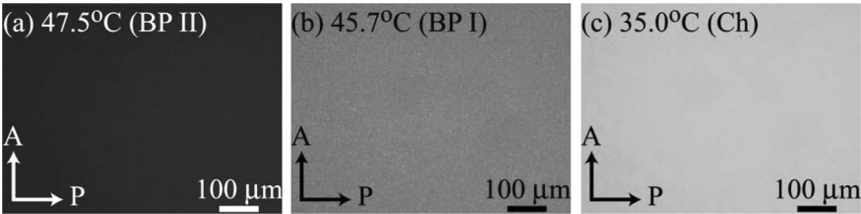


**FIGURE 2** Optical textures of the LC infiltrated in 1-μm MCEM.

in that order with increasing temperature. BP I and BP II exhibit a three-dimensional periodic structure in the director field, having body-centered and simple cubic symmetry, respectively. The lattice periods are comparable to the wavelength of visible light, resulting in the selective Bragg reflection of visible light. BP III is seemingly amorphous with a cubic local structure. Figure 3 shows the reflection spectrum of the LC infiltrated in 1- $\mu\text{m}$  MCEM at various temperatures. Reflection peak was observed at 520 nm (42.0°C) and 430 nm (47.5°C). These reflection peaks could be assigned to be the Bragg diffraction from the (110) plane of the cubic lattice in BP I and from the (100) plane of the cubic lattice in BP II, respectively. Therefore, it is concluded that LC exhibits BP even in the MCEM, although the size of platelets that are characteristic of the BP are small. For the BP LC without MCEM, on slowly cooling (0.01°C/min) LC from the isotropic phase, the size of platelet textures becomes larger than that on faster cooling (1.0°C/min). However, the size of platelet of BP LC infiltrated in the MCEM did not depend on cooling rate. This result indicates that platelet was confined in the voids of MCEM structure.

From the optical textures observation and reflection spectrum measurement, temperature range of the BP of LC in 3- $\mu\text{m}$  MCEM has been estimated during cooling and heating process at the same rate (0.5°C/min), which was summarized in Figure 4. It should be noted that the temperature range of the BP I is drastically expanded (39.4–46.5°C) during cooling process. However this was not observed during heating process. These results indicate that mixed cellulose ester membrane structure causes a pinning effect on appearance of BP I. The temperature range of BP I expanded by the infiltration into

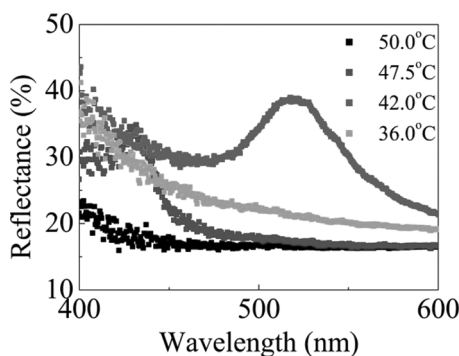


**FIGURE 3** Reflective spectrum of the BP infiltrated in 1- $\mu\text{m}$  MCEM.

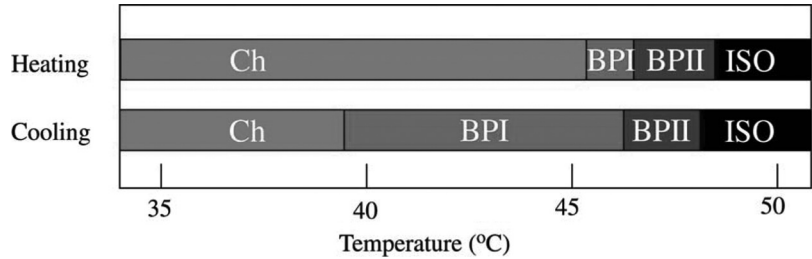


**FIGURE 4** Appearance temperature range of LC phase with 3- $\mu\text{m}$  MCEM during cooling process and heating process.

the MCEM was much wider than the expanded temperature range by the super cooling of BP LC without MCEM [17].

The effect of the network morphology of MCEM to the BP expansion has been investigated. Figure 5 shows SEM images of 1- $\mu\text{m}$  MCEM before and after solvent treatment. After the solvent treatment, mixed cellulose ester network became thin. Figure 6 shows temperature range of BPs infiltrated in 1- $\mu\text{m}$  MCEM with and without solvent treatment. BP I temperature range of the LC infiltrated in MCEM with solvent treatment was wider than that in the MCEM without solvent treatment. This result indicates that thinner network leads bigger expansion of BP I temperature range of LC infiltrated in MCEM.

The cooling rate dependence of the BP I temperature range of the LC infiltrated in MCEM having 3- $\mu\text{m}$  and 0.3- $\mu\text{m}$  pore size is shown in Figure 7. The BP I temperature range depends on the cooling rate, while that of BP II stayed constant. When the cooling rate

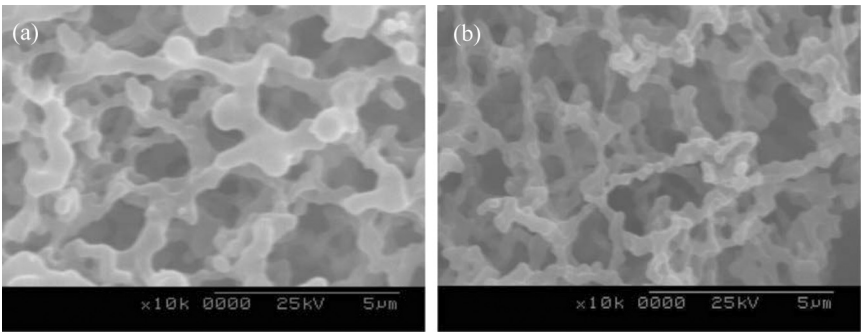


**FIGURE 5** SEM images of 1- $\mu\text{m}$  MCEM (a) before solvent treatment and (b) after solvent treatment.

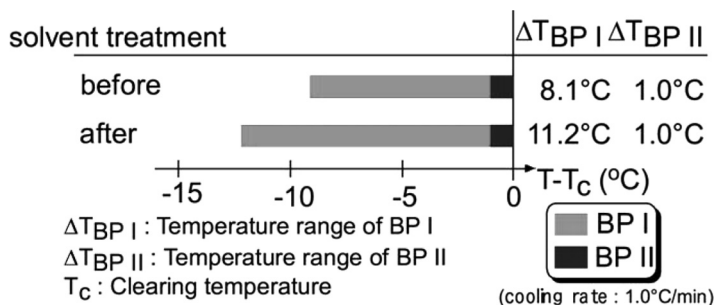


**FIGURE 6** Appearance temperature range of BPs with 1- $\mu$ m MCEM before and after solvent treatment.

is enormously low, temperature range of BP with MCEM is approximately the same as that of BP LC without MCEM. These results also indicate that the expanded BP in the MCEM is not thermodynamically stable and temperature range of BP in MCEM is expanded by pinning effect of membrane structure. The slope of cooling rate dependence should indicate the pinning power. The pinning power of 0.3- $\mu$ m MCEM was larger than that of 3.0- $\mu$ m MCEM, because the slope of cooling rate dependence of 0.3- $\mu$ m MCEM was larger than that of 3.0- $\mu$ m MCEM. Therefore it may be considered that smaller pore size of MCEM leads larger pinning effect. More smaller pore size MCEM infiltrated with BPs is now understudied.

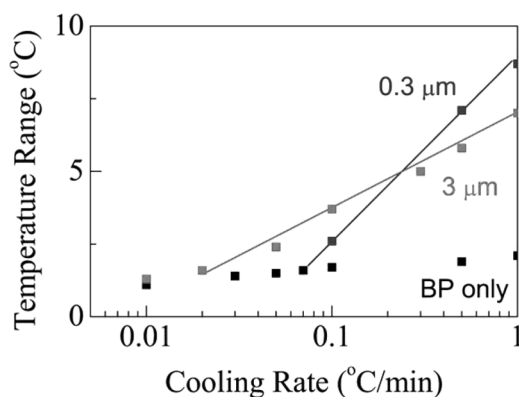


**FIGURE 7** Cooling rate dependence of the temperature range of BP I infiltrated in MCEM with 3- $\mu$ m and 0.3- $\mu$ m pore size.



## CONCLUSION

Temperature range of BP I was expanded at cooling stage by infiltrating BPs in to the MCEM. On the heating stage, there is no expansion of appearance temperature range of BPs. Thin network of MCEM with solvent treatment of aqueous solution of ethanol leads wider expansion of appearance temperature range of BP I. The expansion temperature range depended on cooling rate. Therefore we considered that this expansion of temperature range was induced by the pinning effect on the surface of MCEM. The pinning effect became larger with smaller pore size of MCEM.

## REFERENCES

- [1] Wright, D. C. & Mermin, N. D. (1989). *Rev. Mod. Phys.*, **61**, 385.
- [2] Johnson, D. L., Flack, J. H., & Crooker, P. P. (1980). *Phys. Rev. Lett.*, **45**, 641.
- [3] Meiboom, S., Sammon, M., & Brinkman, W. F. (1983). *Phys. Rev. A*, **27**, 438.
- [4] Etchegoin, P. (2000). *Phys. Rev. E*, **62**, 1435.
- [5] Cao, W., Munoz, A., Palfy-Muhoray, P., & Taheri, B. (2002). *Nat. Mater.*, **1**, 111.
- [6] Yokoyama, S., Mashiko, S., Kikuchi, H., Uchida, K., & Nagamura, T. (2006). *Adv. Mater.*, **18**, 48.
- [7] Hisakado, Y., Kikuchi, H., Nagamura, T., & Kajiyama, T. (2005). *Adv. Mater.*, **17**, 2311.
- [8] Haseba, Y., Kikuchi, H., Nagamura, T., & Kajiyama, T. (2005). *Adv. Mater.*, **17**, 2311.
- [9] Haseba, Y. & Kikuchi, H. (2007). *Mol. Cryst. Liq. Cryst.*, **470**, 1.
- [10] Kikuchi, H., Yokota, M., Hisakado, Y., Yang, H., & Kajiyama, T. (2002). *Nat. Mater.*, **1**, 64.
- [11] Coles, H. J. & Pivnenko, M. N. (2005). *Nature*, **436**, 997.
- [12] Yoshizawa, A., Sato, M., & Rokunohe, J. (2005). *J. Mater. Chem.*, **15**, 3285.
- [13] Noma, T., Ojima, M., Asagi, H., Kawahira, Y., Fujii, A., Ozaki, M., & Kikuchi, H. (2008). *e-J. Surf. Sci. Nanotech.*, **6**, 17.
- [14] Bellini, T., Clark, N. A., Muzny, C. D., Wu, L., Garland, C. W., Schaefer, D. W., & Oliver, B. J. (1992). *Phys. Rev. Lett.*, **69**, 788.
- [15] Wittebrood, M. M., Luijendijk, D. H., Stallinga, S., Rasing, T. H., & Musevic, I. (1996). *Phys. Rev. E*, **54**, 5232.
- [16] Boamfa, M. I., Kim, M. W., Maan, J. C., & Rasing, Th. (2003). *Nature*, **421**, 149.
- [17] Demikhov, E., Stegemeyer, H., & Tsukruk, V. (1992). *Phys. Rev. A*, **46**, 4879–4887.